Full Paper

Design and Synthesis of Benzimidazole Analogs Endowed with Oxadiazole as Selective COX-2 Inhibitor

Ankita Rathore[1], Mujeeb Ur Rahman[1], Anees Ahamad Siddiqui[1], Abuzer Ali[2], and Mohammad Shaharyar[1]

[1] Faculty of Pharmacy, Department of Pharmaceutical Chemistry, Jamia Hamdard (Hamdard University), New Delhi, India
[2] Faculty of Pharmacy, Phytochemistry Research Laboratory, Jamia Hamdard (Hamdard University), New Delhi, India

New molecules of benzimidazole endowed with oxadiazole were designed and synthesized from 2-(2-((pyrimidin-2-ylthio)methyl)-1*H*-benzo[*d*]imidazol-1-yl)acetohydrazide as 1-((5-substituted alkyl/aryl-1,3,4-oxadiazol-2-yl)methyl)-2-((pyrimidin-2-ylthio)methyl)-1*H*-benzimidazoles (**5a–r**) with the aim to acquire selective cyclooxygenase (COX-2) inhibitor activity. The synthesized compounds were screened by *in vitro* cyclooxygenase assays to determine COX-1 and COX-2 inhibitory potency and the results showed that they had good-to-remarkable activity with an IC_{50} range of 11.6–56.1 μM. The most active compounds were further screened for their *in vivo* anti-inflammatory activity by using the carrageenan-induced rat paw edema model. *In vitro* anticancer activities of the hybrid compounds were assessed by the National Cancer Institute (NCI), USA, against 60 human cell lines, and the results showed a good spectrum. Compound **5l** exhibited significant COX-2 inhibition with an IC_{50} value of 8.2 μM and a percent protection of 68.4%. Compound **5b** evinced moderate cytotoxicity toward the UO-31 cell line of renal cancer. A docking study was performed using Maestro 9.0, to provide the binding mode into the binding sites of the cyclooxygenase enzyme. Hopefully, in the future, compound **5l** could serve as a lead compound for developing new COX-2 inhibitors.

Keywords: Benzimidazole / Cyclooxygenase 1 and 2 / Indomethacin / Oxadiazole / Selectivity index

Received: June 8, 2014; Revised: July 28, 2014; Accepted: August 15, 2014

DOI 10.1002/ardp.201400219

Introduction

Inflammation is a biological response of vascular tissues to harmful stimuli, such as pathogens, damaged cells, or irritants [1, 2]. Non-steroidal anti-inflammatory drugs (NSAIDs) are preferably used as therapeutic agents for a variety of inflammatory disorders [3]. Nevertheless, the extensive use of these drugs is limited due to their severe toxicity such as gastrointestinal, ulcerogenicity, GI bleeding, renal irritation, and asthmatic reactions [4–6]. Most of the NSAIDs exert their main biological effects by inhibition of unwanted COX-1 and desired inhibition of the COX-2. The clinical use of selective COX-2 inhibitors has been eliminated due to their undesirable cardiovascular effects, which certainly necessitate the need to investigate new scaffolds possessing COX-2 inhibitory potential [7]. Recent studies have showed that the stimulation of pro-mitogenic factors, carcinogenesis, and tumor angiogenesis leads to upregulation of COX-2 enzyme, eventually ending up in significant clinical concerns [8–11]. Consequently, the suppressive and preventive effects of COX-2 activity on the various types of a cancer subpanel like colon, lung, gastric, and intestinal cancer have been widely studied [12–14].

Among the heterocyclic compounds benzimidazole is an overwhelming pharmacophore and privileged structure that has variety of medicine worldwide in market. From the reported literature, benzimidazoles indicated promising pharmacological activities, viz. anticancer [15], analgesic [16], anti-inflammatory [17], COX-2 inhibitory [18–20], anthelminthic

Correspondence: Dr. Mohammad Shaharyar, Faculty of Pharmacy, Department of Pharmaceutical Chemistry, Jamia Hamdard (Hamdard University), Hamdard Nagar, New Delhi 110062, India
E-mail: yarmsy@rediffmail.com
Fax: +91 11 16988874

© 2014 WILEY-VCH Verlag GmbH & Co. KGaA, Weinheim

(mebendazole), antihypertensive (candesartan), antipsychotic (pimozide), proton pump inhibitory (omeprazole), and ion-dilatory (pimobendan). In order to make high potency drug molecules, one of the strategies would be to combine two bioactive molecules belonging to a particular therapeutic category. This approach is gaining importance in therapeutic categories such as cytotoxicity and anti-inflammatory areas [21–23]. Recent trends in medicinal chemistry showed the popularity of molecular hybridization for drug design and development, which is based on combination of pharmacophoric moieties of different bioactive substances to make a new hybrid molecule with improved affinity and efficacy, as compared to parent drug [24–26]. Some reported biologically active agents, which contains benzimidazole residue and other related heterocyclic moieties, for example, celecoxib, mebendazole, indomethacin, and omeprazole and similarly designed hybrid molecules (**5a–r**) are structurally shown in Scheme 1.

These facts prompted us to synthesize and evaluate a new series of benzimidazole derivatives with the hope of discovering compounds possessing significant COX-2 inhibitory potential. The involvement of COX-2 in the propagation of cancer and the evaluations of several COX-2 inhibitors for reducing cancer propagation impelled us to investigate the present compounds for their anticancer activities.

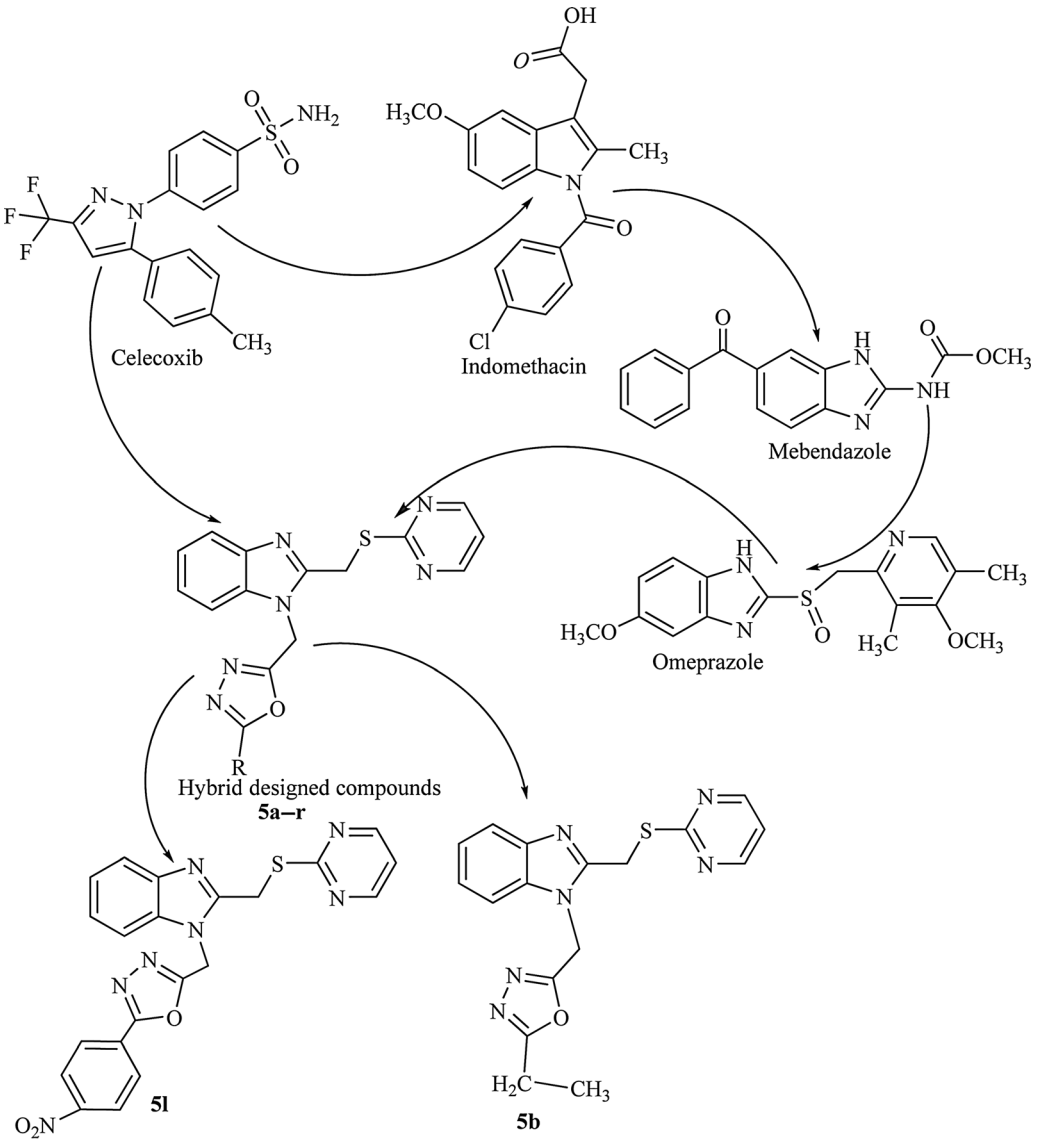

Scheme 1. Rationale of designing the template for the targeted hybrid molecules (**5a–r**) obtained from marketed drugs like celecoxib, mebendazole, indomethacin, and omeprazole and similarly designed hybrid molecules (**5l** and **5b**).

© 2014 WILEY-VCH Verlag GmbH & Co. KGaA, Weinheim

Results and discussion

Chemistry

The synthetic strategy has been explored, to obtain title compounds (**5a–r**) in excellent yield with economical cost, according to the sequence of reactions delineated in Scheme 2. The first step of the synthesis involved preparation of 2-(chloromethyl)-1*H*-benzimidazole (**1**) as reported [27–29], which was subsequently treated with 2-mercaptopyrimidine to afford 2-((pyrimidin-2-ylthio)methyl)-1*H*-benzimidazole (**2**). Nucleophilic substitution of compound **2** with ethyl chloroacetate in presence of K_2CO_3 yielded ethyl 2-(2-((pyrimidin-2-ylthio)methyl)-1*H*-benzo[*d*]imidazol-1-yl)acetate (**3**). Compound **3** was treated with hydrazine hydrate to obtain 2-(2-((pyrimidin-2-ylthio)methyl)-1*H*-benzo[*d*]imidazol-1-yl)acetohydrazide (**4**). 1-((5-Substituted alkyl/aryl-1,3,4-oxadiazol-2-yl)-methyl)-2-((pyrimidin-2-ylthio)methyl)-1*H*-benzo[*d*]imidazoles (**5a–r**) were prepared by the cyclization of compound **4** with respective carboxylic acids.

The elemental analysis and spectral data (IR, ^{1}H NMR, ^{13}C NMR, and mass) of all the synthesized compounds were found in full agreement with the proposed structures.

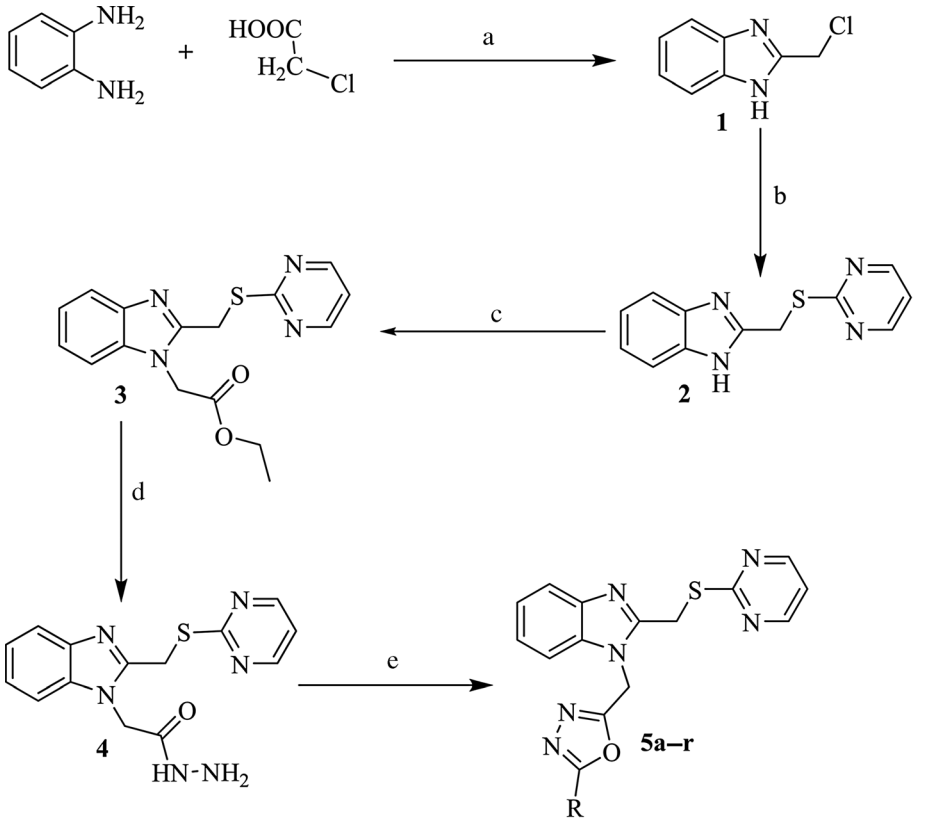

Compd.	-R	Compd.	-R	Compd.	-R
5a	$-CH_3$	**5g**	$2-ClC_6H_4$	**5m**	$2-OHC_6H_4$
5b	$-CH_2CH_3$	**5h**	$4-ClC_6H_4$	**5n**	$4-OHC_6H_4$
5c	$-CH_2Cl$	**5i**	$2-FC_6H_4$	**5o**	$2-CH_3C_6H_4$
5d	$-CH_2CH_2Cl$	**5j**	$4-FC_6H_4$	**5p**	$4-CH_3C_6H_4$
5e	$-CH_2NH_2$	**5k**	$2-NO_2C_6H_4$	**5q**	$2-OCH_3C_6H_4$
5f	$-C_6H_5$	**5l**	$4-NO_2C_6H_4$	**5r**	$4-OCH_3C_6H_4$

Reactions and conditions:
(a) 4 N HCl, 4 h, reflux; (b) 2-mercaptopyrimidine/tetrahydrofuran/TEA, 24 h, stir; (c) ethyl chloroactate/dry acetone/K_2CO_3, reflux, 8 h; (d) $NH_2NH_2.H_2O$/methanol, reflux, 6 h; (e) $POCl_3$, substituted carboxylic acid, reflux, 10–12 h.

Scheme 2. Synthetic protocol for the title compounds **5a–r**.

© 2014 WILEY-VCH Verlag GmbH & Co. KGaA, Weinheim

^{1}H NMR spectral peaks of the respective protons of the synthesized compounds were verified on the basis of their chemical shifts (δ) and multiplicities. The structure was further supported by ^{13}C NMR spectra, which showed peaks at δ 173–166 for carbonyl group, δ 170–159 for oxadiazole carbon, and δ 159–151 for C=N. The mass spectra (ESI-MS) showed the presence of peak at definite *m/z* value in accordance to the molecular formula. The elemental analysis results were found to be within ±0.4% deviation from the theoretical values for each element analyzed (C, H, and N).

Biological evaluation

In vitro COX inhibition

The synthesized compounds were screened to inhibit ovine COX-1 and human recombinant COX-2. The IC_{50} (μM) values were determined, which is the concentration of compound that affords 50% inhibition of COX-2 for average of two determinations (Table 1). In the assay system, the IC_{50} values of celecoxib on COX-1 and COX-2 were found to be 9.4 and 0.08 μM, respectively, indicating that celecoxib is a selective COX-2 inhibitor [COX-2 (SI) 117.5]. The data of *in vitro* COX-1/COX-2 isozyme inhibition studies revealed that most of the compounds were more selective toward COX-2 (IC_{50} 8.2–22.6 μM; Fig. 1) than COX-1 ($IC_{50} > 100$ μM). Compound **5l** was found the most potent inhibitor of all the synthetic compounds with the greater COX-2 potency and selectivity ($IC_{50} = 8.2$ μM and SI >12.1) as shown in Table 1. It was found that compounds **5h**, **5j**, and **5k** showed moderate inhibition toward COX-2 ($IC_{50} = 22.6$, 11.6, and 14.3 μM). The effects of substituents introduced into the aromatic moiety of synthetic compounds **5g–r** were revealed to be directly dependent on the electronic nature of the substituent. It was inferred from the structure–activity relationship studies that the electron-withdrawing groups were determinants of COX-2 inhibitory potency and COX-2 selectivity index. The compounds **5m–r** having electron-releasing substituents were found the least potent inhibitors as compared to electron-withdrawing counterparts (**5g–l**), with minimum COX-2 potency ($IC_{50} = 61.6$ to >100 μM range) and COX-2 selectivity index. The order of COX-2 selectivity profile was found as p-NO_2 > p-F > o-NO_2 > p-Cl > o-F > o-Cl > p-OCH_3 > o-OCH_3 > o-CH_3 > p-OH > p-CH_3 > o-OH. Compounds **5a–e** displayed moderate inhibitory potency toward COX-2 ($IC_{50} = 20.0$–56.1 μM) and order of activity profile was ethyl > chloroethyl > methylamine > chloromethyl > methyl substituents.

In vivo anti-inflammatory activity

Compounds exhibiting good COX-2 inhibitory activity were further screened for *in vivo* anti-inflammatory activity. The results of anti-inflammatory activities against carrageenan-induced rat paw edema of selected compounds are shown in Table 2. Among six compounds, three compounds were proved to have promising anti-inflammatory activity in comparison to standard drug indomethacin. Compound **5l** exhibited maximum anti-inflammatory activity (68.4%) and proved to be the most potent compound of the series. Compounds **5b** and **5j** were found to provide notable protection against inflammation of 59.2 and 65.2% in comparison to standard drug (indomethacin), which has a percent protection of 57.9%. The compounds **5h**, **5i**, and **5k** also showed significant percent inhibition compared to indomethacin (52.8, 54.3 and 56.7%). From the obtained result, it is concluded that the selected compounds exhibiting

Table 1. *In vitro* inhibitory concentration (IC_{50}) of COX-1 and COX-2 enzyme and selectivity index (SI) COX-2.

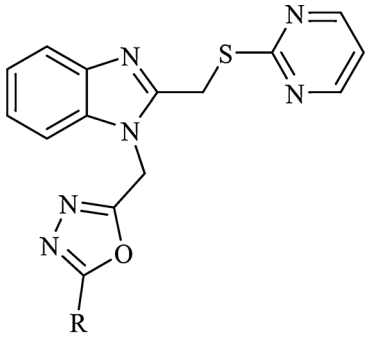

5a–r

Compd. no.	Substituted value (−R)	IC_{50} (μM)[a] COX-1	COX-2	SI[b]
5a	$-CH_3$	>100	56.1	1.7
5b	$-CH_2CH_3$	>100	20.0	5.0
5c	$-CH_2Cl$	78.0	50.2	1.5
5d	$-CH_2CH_2Cl$	>100	38.3	2.6
5e	$-CH_2NH_2$	>100	44.0	2.2
5f	$-C_6H_5$	>100	40.4	2.4
5g	o-ClC_6H_4	87.6	30.6	2.8
5h	p-ClC_6H_4	>100	22.6	4.4
5i	o-FC_6H_4	82.9	26.1	3.1
5j	p-FC_6H_4	>100	11.6	8.6
5k	o-$NO_2C_6H_4$	>100	14.3	6.9
5l	p-$NO_2C_6H_4$	>100	8.2	12.1
5m	o-OHC_6H_4	>100	>100	>1.0
5n	p-OHC_6H_4	>100	83.4	>1.1
5o	o-$CH_3C_6H_4$	>100	71.2	>1.4
5p	p-$CH_3C_6H_4$	>100	85.6	>1.1
5q	o-$OCH_3C_6H_4$	>100	68.4	>1.4
5r	p-$OCH_3C_6H_4$	>100	61.6	>1.6
Celecoxib	–	9.4	0.08	117.5
Indomethacin	–	0.20	6.2	0.03

[a] IC_{50} value: concentration of compounds required to produce 50% inhibition of ovine COX-1 or human recombinant COX-2 for means of two determinations using the enzyme immunoassay kit.

[b] *In vitro* COX-2 selectivity index (COX-1 IC_{50}/COX-2 IC_{50}).

© 2014 WILEY-VCH Verlag GmbH & Co. KGaA, Weinheim

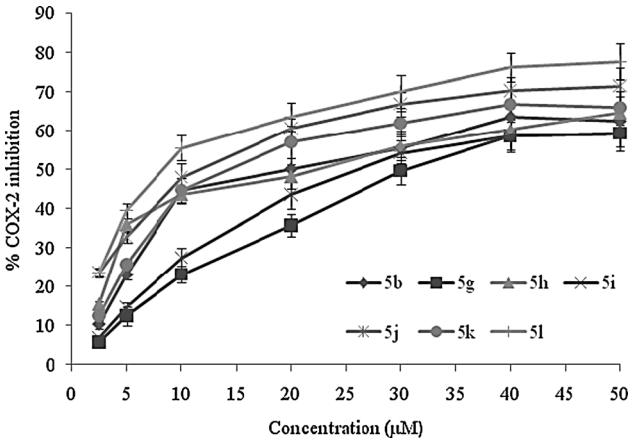

Figure 1. Percentage inhibition of the COX-2 enzyme for potent compounds (**5b**, **5g**, **5h**, **5i**, **5j**, **5k**, and **5l**) at different concentrations.

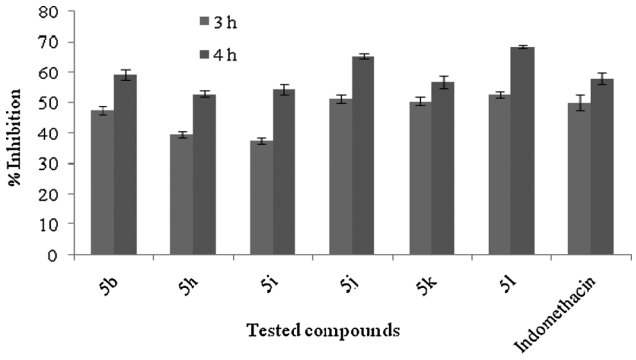

Figure 2. Percentage inhibition of the tested compounds (**5b**, **5h**, **5i**, **5j**, **5k**, and **5l**) on the carrageenan-induced rat paw edema.

significant COX-2 inhibition proved to have promising anti-inflammatory activity. The percentage anti-inflammatory activity of tested compounds at different time intervals is shown in Fig. 2.

Acute ulcerogenicity study

The tested compounds that exhibited significant anti-inflammatory activity in comparison to standard drug indomethacin were screened for their ulcerogenic potential. The results of these investigations indicated that all the tested compounds exhibited a superior GI safety profile (SI values 0.48–0.62) in Wistar rats as compared to standard drug indomethacin (SI value 1.96 ± 0.13) (Table 2). Most active compounds **5j** and **5l** exhibited a severity index of 0.54 ± 0.30 and 0.48 ± 0.20, which is very less than the value obtained with the standard drug. These findings suggested that these compounds may be considered safer in terms of gastric toxicity than the standard drug indomethacin.

Lipid peroxidation study

In order to validate the results of ulcerogenicity, compounds were further subjected to lipid peroxidation studies and results are tabulated in Table 2. All the tested compounds have shown marked reduction in lipid peroxidation (a range of 4.79–5.10 nM of MDA formed/h/mg of protein). It is meaningful to mention that indomethacin displayed the highest lipid peroxidation, 6.98 ± 0.40 nM of MDA formed/h/mg of protein, whereas the control group showed a lipid peroxidation of 3.51 ± 0.28 nM of MDA formed/h/mg of protein under the same experiment conditions.

Table 2. *In-vivo* anti-inflammatory inhibition of compounds **5b**, **5h**, **5i**, **5j**, **5k**, and **5l** by using carrageenan-induced rat paw edema model.

Compd. no.	Paw volume (mL) (mean ± SEM) [a]		% Inhibition ± SEM		Ulcerogenic activity (SI[b]) (mean ± SEM)[c]	nM of MDA formed/h/mg of protein (mean ± SEM)[c]
	3 h	4 h	3 h	4 h		
Control	1.92 ± 0.05	2.76 ± 0.07	–	–	0.00 ± 00	3.51 ± 0.28
5b	1.00 ± 0.02	1.12 ± 0.04	$47.6 \pm 1.3^{**}$	$59.2 \pm 1.6^{**}$	$0.62 \pm 0.26^{**}$	$5.10 \pm 0.30^{**}$
5h	1.16 ± 0.02	1.30 ± 0.04	$39.5 \pm 1.1^{**}$	$52.8 \pm 1.0^{**}$	–	–
5i	1.20 ± 0.06	1.26 ± 0.02	$37.5 \pm 1.0^{**}$	$54.3 \pm 1.7^{**}$	–	–
5j	0.93 ± 0.02	0.96 ± 0.04	$51.3 \pm 1.1^{**}$	$65.2 \pm 0.9^{**}$	$0.54 \pm 0.30^{**}$	$4.92 \pm 0.38^{**}$
5k	0.95 ± 0.04	1.19 ± 0.05	$50.5 \pm 1.2^{**}$	$56.7 \pm 2.0^{**}$	–	–
5l	0.90 ± 0.02	0.86 ± 0.01	$52.6 \pm 1.1^{**}$	$68.4 \pm 0.5^{**}$	$0.48 \pm 0.20^{**}$	$4.79 \pm 0.27^{**}$
Indomethacin	0.96 ± 0.04	1.16 ± 0.04	$50.0 \pm 2.4^{**}$	$57.9 \pm 1.9^{**}$	1.96 ± 0.13	6.98 ± 0.40

[a] Data were analyzed by ANOVA followed by Dunnett's multiple comparison test ($n = 6$). $^{**}p < 0.01$, compared to control.
[b] Severity index (SI): Score of each treated group minus the mean score of the control group.
[c] Relative to standard and data were analyzed by ANOVA followed by Dunnett's multiple comparison test ($n = 6$). $^{**}p < 0.01$, compared to standard.

© 2014 WILEY-VCH Verlag GmbH & Co. KGaA, Weinheim

In vitro anticancer activity

In vitro anticancer activity screening of synthesized compounds was performed by National Cancer Institute (NCI), USA. As per the protocol of NCI, selected compounds of the series were granted NSC code as NSC D-772603/1 (**5a**), NSC D-772604/1 (**5b**), NSC D-772605/1 (**5f**), NSC D-772606/1 (**5h**), NSC D-772607/1 (**5j**), NSC D-772609/1 (**5n**), and NSC D-772608/1 (**5r**) and screened for *in vitro* anticancer activity at a single dose (10 μM) against NCI 60 cell panel. Among all the tested compounds, four compounds were found active *in vitro* and showed good-to-moderate growth inhibition. Compounds **5b**, **5h**, **5j**, and **5r** showed 39.11, 35.67, 34.45, and 32.52% growth inhibition against UO-31 cell lines of renal cancer, respectively (Fig. 3). Furthermore, the mean of growth percent for the compounds **5b**, **5h**, **5j**, and **5r** were found to be 60.89, 64.33, 65.55, and 67.48%, respectively. Compounds **5a**, **5f**, and **5n** did not show significant growth inhibition against any of cancer cell lines. Overall results of the primary *in vitro* anticancer assay showed that the compounds **5b**, **5h**, **5j**, and **5r** were moderately active while compounds **5a**, **5f**, and **5n** were inactive on tested cell lines (Table 3).

Conclusion

The designed compounds were successfully synthesized under mentioned reaction condition and evaluated for their selective COX-2 inhibitory potential and potent compounds were further screened for anti-inflammatory, ulcerogenicity, and lipid peroxidation. The structures of newly synthesized compounds were established on the basis of modern analytical techniques (FT-IR, ^{1}H NMR, ^{13}C NMR, and mass spectrometry). The elemental analysis results were within ±0.4% of the theoretical values and final compounds were found pure on TLC examination. The obtained results of selected compounds showed good-to-significant activity. Among these, compound **5l** was found the most potent and selective COX-2 inhibitor with IC_{50} 8.2 μM as well as promising anti-inflammatory agent (68.4%) and could be emerged as lead compound. The compound **5l** was also proved to be devoid of gastric toxicity in comparison to standard drug indomethacin. Compound **5b** showed dual action with 39.11% inhibition against UO-31 cell line of renal cancer and significant anti-inflammatory potential (COX-2, IC_{50} 20.0 μM; 59.2% inhibition). Furthermore, molecular docking study was performed using Maestro 9.4 program (Schrodinger, Inc., USA) to provide the binding patterns of the compound **5l** into the binding sites of COX-1 and COX-2 (PDB ID: 1PGF and 6COX) and proved the compound more selective for COX-2. In view of these points, the compound **5l** could be a subject of further investigations for searching potential new anti-inflammatory agents and support for the design of new molecules.

Experimental

General methods

Melting points were determined using open capillary tubes on an electrical melting point apparatus and are uncorrected. ^{1}H NMR and ^{13}C NMR spectra were recorded on Bruker spectrospin DPX-400 MHz in $CDCl_3$. Chemical shift (δ) values were reported in parts per million (ppm) using tetramethylsilane as an internal reference. The exchangeable protons (OH and NH) were confirmed by D_2O exchange. Mass spectra were recorded on LC–MS/MS (PerkinElmer and LABINDIA, Applied Biosystem), presented as *m/z*. Elemental analyses were performed on a PerkinElmer 240 analyzer. The progress of the reactions and purity of the synthesized compounds were verified on ascending thin layer chromatography (TLC) plates (silica gel G) and toluene/ethyl acetate/formic acid (6:3:1 v/v/v) was used as solvent system. COX assay kit (catalogue no. 560131) was purchased from Cayman Chemical Company (Ann Arbor, MI, USA).

*2-((Pyrimidin-2-ylthio)methyl)-1H-benzimidazole (**2**)*

A solution of the 2-mercaptopyrimidine (0.01 mol) in dry tetrahydrofuran (THF) (30 mL) containing triethylamine (TEA) (0.2 mL) was stirred for 2 h. A solution of 2-(chloromethyl)-1*H*-benzimidazole (0.01 mol) in dry tetrahydrofuran was then added portionwise and the reaction mixture was stirred at room temperature for additional 24 h, poured onto crushed ice with stirring. The precipitated product was filtered off and recrystallized from ethanol to give compound **2**. Solid, brown; yield: 70%, m.p. (°C): 177–179; ^{1}H NMR ($CDCl_3$): (δ ppm) 8.52 (2H, d, $J = 2.4$ Hz, pyr-H4, pyr-H6), 7.24 (1H, t, pyr-H5), 7.58–7.30 (m, 4H, Ar–H), 4.38 (s, 2H, CH_2); ^{13}C NMR ($CDCl_3$): (δ ppm) 156 (C=N, pyrimidine), 144 (C=N, benzimidazole), 138–120 (Ar–C), 44 (CH_2); ESI MS (*m/z*): 243 $[M+H]^+$. Anal. calcd. for $C_{12}H_{10}N_4S$: C: 59.48, H: 4.16, N: 23.12; Found: C: 59.68, H: 4.17, N: 23.04%.

*Ethyl 2-(2-((pyrimidin-2-ylthio)methyl)-1H-benzo[d]-imidazol-1-yl)acetate (**3**)*

To a solution of 2-((piperidin-1-yl)methyl)-1*H*-benzimidazole (0.01 mol) in dry acetone (30 mL), ethyl chloroacetate (0.01 mol) and anhydrous K_2CO_3 (1 g) were added and the reaction mixture was refluxed for 8 h. After completion of the reaction, K_2CO_3 was removed through filtration. Solvent was evaporated at room temperature. The residue thus obtained was washed with water and crystallized from ethanol to give compound **3**. Solid, dark gray; yield: 62%, m.p. (°C): 153–155; ^{1}H NMR ($CDCl_3$): (δ ppm) 8.40 (2H, d, $J = 2.4$ Hz, pyr-H4, pyr-H6), 7.30 (1H, t, pyr-H5), 7.52–7.20 (m, 4H, Ar-H), 4.70 (s, 2H, CH_2), 4.24 (s, 2H, CH_2), 4.10 (q, 2H, CH_2), 1.26 (t, 3H, CH_3); ^{13}C NMR ($CDCl_3$): (δ ppm) 173 (C=O, ester), 153 (C=N, pyrimidine), 140 (C=N, benzimidazole), 130–121 (Ar–C), 64 (CH_2CH_3), 52 (CH_2COO), 30 (CH_2), 16 (CH_3). ESI MS (*m/z*): 329 $[M+H]^+$. Anal. calcd. for $C_{16}H_{16}N_4O_2S$: C: 58.52, H: 4.91, N: 17.06; Found: C: 58.70, H: 4.90, N: 16.99%.

*2-(2-((Pyrimidin-2-ylthio)methyl)-1H-benzo[d]imidazol-1-yl)acetohydrazide (**4**)*

To a solution of compound **3** (0.01 mol) in methanol (60 mL), 99% hydrazine hydrate (1 mL) was added and the mixture was refluxed for 6 h. The reaction mixture was cooled and the solid thus obtained was filtered, washed with water, and recrystallized with ethanol to afford the compound **4**. Amorphous powder, dark

© 2014 WILEY-VCH Verlag GmbH & Co. KGaA, Weinheim

Developmental Therapeutics Program
One Dose Mean Graph

NSC: D-772604 / 1	Conc: 1.00E-5 Molar	Test Date: Feb 25, 2013
Experiment ID: 1302OS30		Report Date: Apr 26, 2013

Panel/Cell Line	Growth Percent
Leukemia	
CCRF-CEM	101.05
HL-60(TB)	96.96
K-562	105.32
MOLT-4	99.76
RPMI-8226	102.77
SR	102.41
Non-Small Cell Lung Cancer	
A549/ATCC	95.17
HOP-62	93.97
HOP-92	89.67
NCI-H226	99.14
NCI-H23	92.80
NCI-H322M	82.35
NCI-H460	101.65
NCI-H522	88.95
Colon Cancer	
COLO 205	97.24
HCC-2998	103.20
HCT-116	96.01
HCT-15	96.18
HT29	102.24
KM12	98.99
SW-620	94.69
CNS Cancer	
SF-268	97.49
SF-295	94.01
SF-539	88.27
SNB-19	96.83
SNB-75	89.33
U251	93.47
Melanoma	
LOX IMVI	92.00
MALME-3M	87.98
M14	94.67
MDA-MB-435	90.85
SK-MEL-28	99.21
SK-MEL-5	97.56
UACC-257	86.88
UACC-62	95.64
Ovarian Cancer	
IGROV1	81.40
OVCAR-3	97.20
OVCAR-4	102.52
OVCAR-5	103.65
OVCAR-8	84.64
NCI/ADR-RES	99.53
SK-OV-3	91.37
Renal Cancer	
786-0	102.02
A498	131.29
ACHN	97.30
CAKI-1	72.72
RXF 393	107.66
SN12C	97.84
TK-10	128.99
UO-31	60.89
Prostate Cancer	
PC-3	89.88
DU-145	101.15
Breast Cancer	
MCF7	88.52
MDA-MB-231/ATCC	95.61
HS 578T	111.09
BT-549	95.46
T-47D	92.32
MDA-MB-468	102.74
Mean	96.22
Delta	35.33
Range	70.40

Mean Growth Percent - Growth Percent

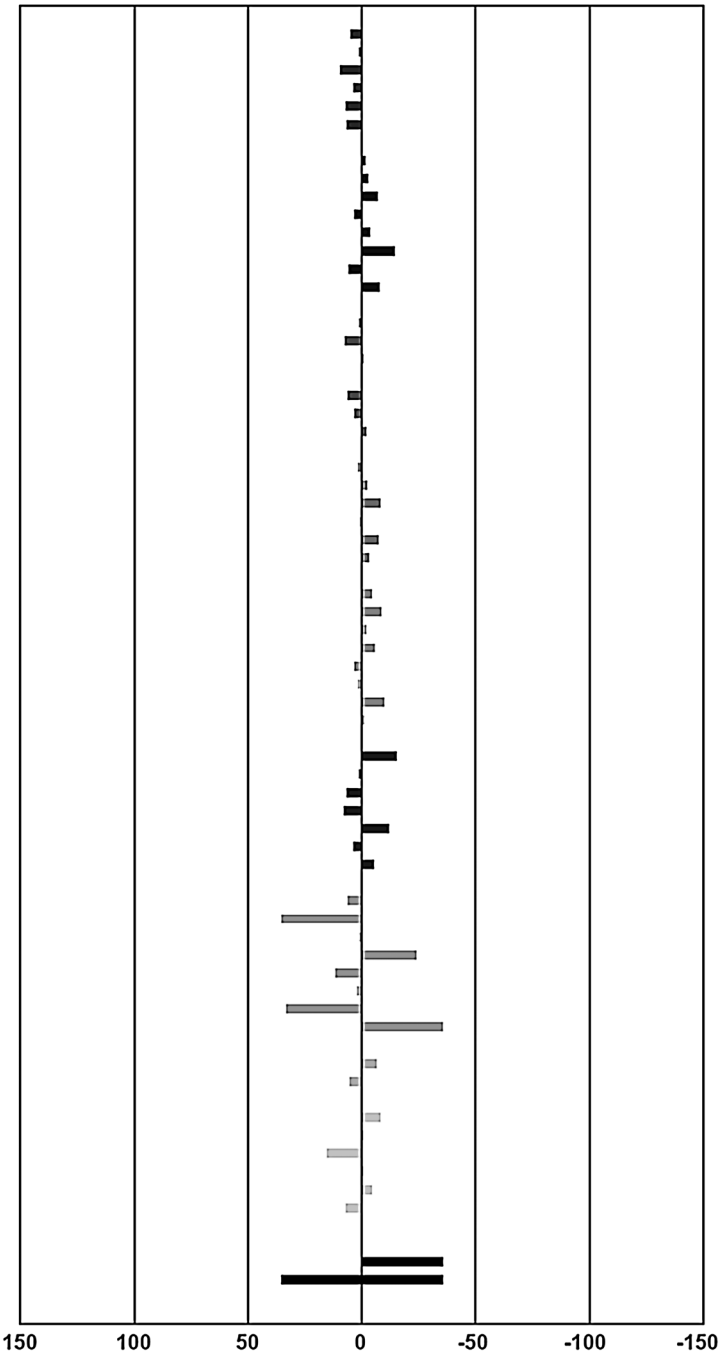

Figure 3. Preliminary screening of compound **5b** at a dose of 1×10^{-5} M against NCI 60 cell lines.

© 2014 WILEY-VCH Verlag GmbH & Co. KGaA, Weinheim

Table 3. Sensitivity, NSC: code, growth percent, delta value, mean growth percent of NCI cancer cell lines treated with compounds **5a**, **5b**, **5f**, **5h**, **5j**, **5n**, and **5r** at a dose of 1×10^{-5} M by NCI.

Compd. no.	NSC: code	The most sensitive cell line	Growth % of the most sensitive cell line	% Growth inhibition	Range of growth %	Mean	Delta	Range	Activity[a)]
5a	772603/1	UO-31 (renal cancer)	71.35	28.65	71.35–132.58	98.21	26.86	61.23	Inactive
5b	772604/1	UO-31 (renal cancer)	60.89	39.11	60.89–128.99	96.22	35.33	70.40	Active
5f	772605/1	UO-31 (renal cancer)	73.54	26.46	73.54–111.90	96.97	23.43	53.35	Inactive
5h	772606/1	UO-31 (renal cancer)	64.33	35.67	64.33–111.96	98.19	33.86	58.17	Active
5j	772607/1	UO-31 (renal cancer)	65.55	34.45	65.55–122.95	101.38	35.83	57.40	Active
5n	772609/1	TK-10 (renal cancer)	75.06	24.94	75.06–119.19	100.94	25.88	44.13	Inactive
5r	772608/1	UO-31 (renal cancer)	67.48	32.52	67.48–126.62	101.52	34.04	59.14	Active

[a)] The compounds which were active for the particular cell lines, which showed growth inhibition ≤32% cell growth reduction following 48-h incubation with test compounds.

gray; yield: 65%, m.p. (°C): 190–192; ^{1}H NMR ($CDCl_3$): (δ ppm) 12.01 (s, 1H, NH, D_2O exchangeable), δ 8.76 (2H, d, $J = 2.4$ Hz, pyr-H4, pyr-H6), 7.18 (1H, t, pyr-H5), 7.88–7.20 (m, 4H, Ar–H), 4.90 (s, 2H, CH_2), 4.28 (s, 2H, CH_2), 4.00 (br, 2H, NH_2, D_2O exchangeable); ^{13}C NMR ($CDCl_3$): (δ ppm) 166 (C=O, hydrazide), 157 (C=N, pyrimidine), 142 (C=N, benzimidazole), 128–115 (Ar–C), 39 ($\underline{C}H_2CO$), 32 (CH_2). ESI MS (*m/z*): 315 $[M+H]^+$. Anal. calcd. for $C_{14}H_{14}N_6OS$: C: 53.49, H: 4.49, N: 26.73; Found: C: 53.66, H: 4.47, N: 26.64%.

*General procedure for the synthesis of 1-((5-substituted alkyl/aryl-1,3,4-oxadiazol-2-yl)methyl)-2-((pyrimidin-2-ylthio)methyl)-1H-benzo[d]imidazoles (**5a–r**)*

An equimolar mixture of compound **4** (0.001 M) and substituted carboxylic acid in 5–6 mL of phosphoryl chloride ($POCl_3$) was refluxed for 10–12 h. Then reaction mixture was cooled, poured into ice-cold water, and neutralized with 20% $NaHCO_3$ solution. The resultant solid was filtered, washed with water, and recrystallized from ethanol to give the title compounds.

*1-[(5-Methyl-1,3,4-oxadiazol-2-yl)methyl]-2-[(pyrimidin-2-ylthio)methyl]-1H-benzo[d]imidazole (**5a**)*

Solid, dark brown; yield: 70%; m.p. (°C): 130–133; IR (KBr) cm^{-1}: 3019 (Ar–H), 2912 (C–CH_3), 2871 (C–H, CH_2), 1662 (C=N benzimidazole), 1571 (C=N pyrimidine), 1548 (C=C), 1366 (C–N), 1138 (C–O–C); ^{1}H NMR ($CDCl_3$): (δ ppm) 8.94 (2H, d, J= 2.4 Hz, pyr-H4, pyr-H6), 7.20 (1H, t, pyr-H5), 7.52–7.31 (m, 4H, Ar–H), 4.80 (s, 2H, CH_2), 4.07 (s, 2H, CH_2), 2.31 (s, 3H, CH_3); ^{13}C NMR ($CDCl_3$): (δ ppm) 164, 161 (2C, oxadiazole), 155 (C=N, pyrimidine), 147 (C=N, benzimidazole), 136–114 (Ar–C), 52 (CH_2), 30 (CH_2), 16 (CH_3); ESI MS (*m/z*): 339 $[M+H]^+$. Anal. calcd. for $C_{16}H_{14}N_6OS$: C: 56.79, H: 4.17, N: 24.84; Found: C: 56.98, H: 4.18, N: 24.77%.

*1-((5-Ethyl-1,3,4-oxadiazol-2-yl)methyl)-2-((pyrimidin-2-ylthio)methyl)-1H-benzo[d]imidazole (**5b**)*

Powder, gray; yield: 71%; m.p. (°C): 207–209; IR (KBr) cm^{-1}: 2998 (Ar–H), 2906 (C–CH_3), 2868 (C–H, CH_2), 1649 (C=N benzimidazole), 1566 (C=N pyrimidine), 1535 (C=C), 1377 (C–N), 1131 (C–O–C); ^{1}H NMR ($CDCl_3$): (δ ppm) 8.73 (2H, d, $J = 2.0$ Hz, pyr-H4, pyr-H6), 7.14 (1H, t, pyr-H5), 7.72–7.28 (m, 4H, Ar–H), 4.66 (s, 2H, CH_2), 4.20 (s, 2H, CH_2), 3.85 (q, 2H, CH_2), 1.48 (s, 3H, CH_3); ^{13}C NMR ($CDCl_3$): (δ ppm) 162, 160 (2C, oxadiazole), 156 (C=N, pyrimidine), 140 (C=N, benzimidazole), 138–117 (Ar–C), 48 (CH_2), 39 (CH_2), 22 (CH_2CH_3), 14 (CH_3). ESI MS (*m/z*): 353 $[M+H]^+$. Anal. calcd. for $C_{17}H_{16}N_6OS$: C: 57.94, H: 4.58, N: 23.85; Found: C: 57.76, H: 4.59, N: 23.90%.

*1-((5-(Chloromethyl)-1,3,4-oxadiazol-2-yl)methyl)-2-((pyrimidin-2-ylthio)methyl)-1H-benzo[d]imidazole (**5c**)*

Solid, dark brown; yield: 66%; m.p. (°C): 162–164; IR (KBr) cm^{-1}: 2995 (Ar–H), 2880 (C–H, CH_2), 1664 (C=N benzimidazole), 1568 (C=N pyrimidine), 1548 (C=C), 1353 (C–N), 1125 (C–O–C); ^{1}H NMR ($CDCl_3$): (δ ppm) 8.70 (2H, d, $J = 2.4$ Hz, pyr-H4, pyr-H6), 7.39 (1H, t, pyr-H5), 7.61–7.22 (m, 4H, Ar–H), 5.18 (s, 2H, CH_2), 4.91 (s, 2H, CH_2Cl), 4.10 (s, 2H, CH_2); ^{13}C NMR ($CDCl_3$): (δ ppm) 162, 160 (2C, oxadiazole), 156 (C=N, pyrimidine), 140 (C=N, benzimidazole), 136–115 (Ar–C), 48 (CH_2Cl), 45 (CH_2), 25 (CH_2); ESI MS (*m/z*): 373 $[M+H]^+$. Anal. calcd. for $C_{16}H_{13}ClN_6OS$: C: 51.54, H: 3.51, N: 22.54; Found: C: 51.70, H: 3.50, N: 22.46%.

*1-((5-(2-Chloroethyl)-1,3,4-oxadiazol-2-yl)methyl)-2-((pyrimidin-2-ylthio)methyl)-1H-benzo[d]imidazole (**5d**)*

Powder, brown; yield: 76%; m.p. (°C): 243–246; IR (KBr) cm^{-1}: 3005 (Ar–H), 2869 (C–H, CH_2), 1664 (C=N benzimidazole), 1577 (C=N pyrimidine), 1560 (C=C), 1382 (C–N), 1149 (C–O–C); ^{1}H NMR ($CDCl_3$): (δ ppm) 9.05 (2H, d, $J = 4.2$ Hz, pyr-H4, pyr-H6), 7.15 (1H, t, pyr-H5), 7.69–7.32 (m, 4H, Ar–H), 4.90 (s, 2H, CH_2), 4.08 (s, 2H, CH_2), 3.98 (t, 2H, CH_2Cl), 2.65 (t, 2H, CH_2); ^{13}C NMR ($CDCl_3$): (δ ppm) 168, 163 (2C, oxadiazole), 158 (C=N, pyrimidine), 146 (C=N, benzimidazole), 139–114 (Ar–C), 45 (CH_2), 43 (CH_2Cl), 31 (CH_2), 28 (CH_2); ESI MS (*m/z*): 387 $[M+H]^+$. Anal. calcd. for $C_{17}H_{15}ClN_6OS$: C: 52.78, H: 3.91, N: 21.72; Found: C: 52.94, H: 3.90, N: 21.66%.

*(5-((2-((Pyrimidin-2-ylthio)methyl)-1H-benzo[d]imidazol-1-yl)methyl)-1,3,4-oxadiazol-2-yl)methanamine (**5e**)*

Amorphous solid, gray; yield: 62%; m.p. (°C): 155–157; IR (KBr) cm^{-1}: 3440, 3360 (C–NH_2), 2980 (Ar–H), 2866 (C–H, CH_2), 1665 (C=N benzimidazole), 1570 (C=N pyrimidine), 1548 (C=C), 1390 (C–N), 1124 (C–O–C); ^{1}H NMR ($CDCl_3$): (δ ppm) 8.98 (2H, d, $J = 2.4$ Hz, pyr-H4, pyr-H6), 7.13 (1H, t, pyr-H5), 7.63–

© 2014 WILEY-VCH Verlag GmbH & Co. KGaA, Weinheim

7.30 (m, 4H, Ar–H), 4.90 (s, 2H, CH_2), 4.84 (s, 2H, CH_2), 3.97 (br, 2H, NH_2, D_2O exchangeable), 2.85 (s, 2H, CH_2); ^{13}C NMR ($CDCl_3$): (δ ppm) 164, 160 (2C, oxadiazole), 157 (C=N, pyrimidine), 149 (C=N, benzimidazole), 133–116 (Ar–C), 45 (CH_2), 43 (CH_2NH_2), 29 (CH_2); ESI MS (*m/z*): 354 $[M+H]^+$. Anal. calcd. for $C_{16}H_{15}N_7OS$: C: 54.38, H: 4.28, N: 27.74; Found: C: 54.19, H: 4.29, N: 27.83%.

*1-((5-Phenyl-1,3,4-oxadiazol-2-yl)methyl)-2-((pyrimidin-2-ylthio)methyl)-1H-benzo[d]imidazole (**5f**)*

Solid, brown; yield: 68%; m.p. (°C): 219–222; IR (KBr) cm^{-1}: 2986 (Ar–H), 2861 (C–H, CH_2), 1647 (C=N benzimidazole), 1577 (C=N pyrimidine), 1568 (C=C), 1352 (C–N), 1134 (C–O–C); ^1H NMR ($CDCl_3$): (δ ppm) 9.08 (2H, d, $J = 2.8$ Hz, pyr-H4, pyr-H6), 7.09 (1H, t, pyr-H5), 7.88–7.28 (m, 9H, Ar–H), 4.38 (s, 2H, CH_2), 4.19 (s, 2H, CH_2); ^{13}C NMR ($CDCl_3$): (δ ppm) 162, 161 (2C, oxadiazole), 159 (C=N, pyrimidine), 141 (C=N, benzimidazole), 134–116 (Ar–C), 48 (CH_2), 33 (CH_2); ESI MS (*m/z*): 401 $[M+H]^+$. Anal. calcd. for $C_{21}H_{16}N_6OS$: C: 62.98, H: 4.03, N: 20.99; Found: C: 63.11, H: 4.04, N: 20.92%.

*1-((5-(2-Chlorophenyl)-1,3,4-oxadiazol-2-yl)methyl)-2-((pyrimidin-2-ylthio)methyl)-1H-benzo[d]imidazole (**5g**)*

Solid powder, dark brown; yield: 60%; m.p. (°C): 275–277; IR (KBr) cm^{-1}: 2999 (Ar–H), 2882 (C–H, CH_2), 1664 (C=N benzimidazole), 1582 (C=N pyrimidine), 1565 (C=C), 1380 (C–N), 1129 (C–O–C), 755 (Ar–Cl); ^1H NMR ($CDCl_3$): (δ ppm) 8.77 (2H, d, $J = 2.4$ Hz, pyr-H4, pyr-H6), 7.12 (1H, t, pyr-H5), 7.83–7.08 (m, 8H, Ar–H), 4.99 (s, 2H, CH_2), 4.12 (s, 2H, CH_2); ^{13}C NMR ($CDCl_3$): (δ ppm) 170, 163 (2C, oxadiazole), 152 (C=N, pyrimidine), 148 (C=N, benzimidazole), 134 (C–Cl), 131–112 (Ar–C), 44 (CH_2), 36 (CH_2); ESI MS (*m/z*): 435 $[M+H]^+$. Anal. calcd. for $C_{21}H_{15}ClN_6OS$: C: 58.00, H: 3.48, N: 19.32; Found: C: 58.22, H: 3.49, N: 19.26%.

*1-((5-(4-Chlorophenyl)-1,3,4-oxadiazol-2-yl)methyl)-2-((pyrimidin-2-ylthio)methyl)-1H-benzo[d]imidazole (**5h**)*

Powder, brown; yield: 69%; m.p. (°C): 133–136; IR (KBr) cm^{-1}: 2995 (Ar–H), 2870 (C–H, CH_2), 1664 (C=N benzimidazole), 1579 (C=N pyrimidine), 1567 (C=C), 1353 (C–N), 1128 (C–O–C), 761 (Ar–Cl); ^1H NMR ($CDCl_3$): (δ ppm) 8.79 (2H, d, $J = 3.4$ Hz, pyr-H4, pyr-H6), 7.18 (1H, t, pyr-H5), 7.82–7.32 (m, 8H, Ar–H), 4.95 (s, 2H, CH_2), 4.33 (s, 2H, CH_2); ^{13}C NMR ($CDCl_3$): (δ ppm) 169, 162 (2C, oxadiazole), 156 (C=N, pyrimidine), 148 (C=N, benzimidazole), 137 (C–Cl), 138–113 (Ar–C), 49 (CH_2), 30 (CH_2); ESI MS (*m/z*): 435 $[M+H]^+$. Anal. calcd. for $C_{21}H_{15}ClN_6OS$: C: 58.00, H: 3.48, N: 19.32; Found: C: 57.80, H: 3.47, N: 19.38%.

*1-((5-(2-Fluorophenyl)-1,3,4-oxadiazol-2-yl)methyl)-2-((pyrimidin-2-ylthio)methyl)-1H-benzo[d]imidazole (**5i**)*

Solid powder, greenish; yield: 63%; m.p. (°C): 186–189; IR (KBr) cm^{-1}: 3013 (Ar–H), 2905, 2880 (C–H, CH_2), 1667 (C=N benzimidazole), 1568 (C=N pyrimidine), 1554 (C=C), 1359 (C–N), 1224 (Ar–F), 1144 (C–O–C); ^1H NMR ($CDCl_3$): (δ ppm) 8.41 (2H, d, $J = 3.4$ Hz, pyr-H4, pyr-H6), 6.96 (1H, t, pyr-H5), 7.79–7.22 (m, 8H, Ar–H), 4.55 (s, 2H, CH_2), 4.14 (s, 2H, CH_2); ^{13}C NMR ($CDCl_3$): (δ ppm) 163, 159 (2C, oxadiazole), 155 (C=N, pyrimidine), 140 (C=N, benzimidazole), 136–116 (Ar–C), 45 (CH_2), 37 (CH_2); ESI MS (*m/z*): 419 $[M+H]^+$. Anal. calcd. for $C_{21}H_{15}FN_6OS$: C: 60.28, H: 3.61, N: 20.08; Found: C: 60.50, H: 3.62, N: 20.15%.

*1-((5-(4-Fluorophenyl)-1,3,4-oxadiazol-2-yl)methyl)-2-((pyrimidin-2-ylthio)methyl)-1H-benzo[d]imidazole (**5j**)*

Solid, cyan; yield: 69%; m.p. (°C): 149–152; IR (KBr) cm^{-1}: 2993 (Ar–H), 2990, 2882 (C–H, CH_2), 1643 (C=N benzimidazole), 1571 (C=N pyrimidine), 1558 (C=C), 1353 (C–N), 1227 (Ar–F), 1126 (C–O–C); ^1H NMR ($CDCl_3$): (δ ppm) 8.72 (2H, d, $J = 2.8$ Hz, pyr-H4, pyr-H6), 7.04 (1H, t, pyr-H5), 7.79–7.27 (m, 8H, Ar–H), 4.95 (s, 2H, CH_2), 4.32 (s, 2H, CH_2); ^{13}C NMR ($CDCl_3$): (δ ppm) 166, 160 (2C, oxadiazole), 155 (C=N, pyrimidine), 145 (C=N, benzimidazole), 132–112 (Ar–C), 49 (CH_2), 32 (CH_2); ESI MS (*m/z*): 419 $[M+H]^+$. Anal. calcd. for $C_{21}H_{15}FN_6OS$: C: 60.28, H: 3.61, N: 20.08; Found: C: 60.08, H: 3.62, N: 19.99%.

*1-((5-(2-Nitrophenyl)-1,3,4-oxadiazol-2-yl)methyl)-2-((pyrimidin-2-ylthio)methyl)-1H-benzo[d]imidazole (**5k**)*

Powder, gray; yield: 62%; m.p. (°C): 256–258; IR (KBr) cm^{-1}: 3018 (Ar–H), 2883 (C–H, CH_2), 1672 (C=N benzimidazole), 1566 (C=N pyrimidine), 1548 (C=C), 1532, 1460 (NO_2), 1356 (C–N), 1125 (C–O–C); ^1H NMR ($CDCl_3$): (δ ppm) 8.92 (2H, d, $J = 3.6$ Hz, pyr-H4, pyr-H6), 7.01 (1H, t, pyr-H5), 7.83–7.25 (m, 8H, Ar–H), 4.81 (s, 2H, CH_2), 4.33 (s, 2H, CH_2); ^{13}C NMR ($CDCl_3$): (δ ppm) 168, 163 (2C, oxadiazole), 157 (C=N, pyrimidine), 148 (C–NO_2), 141 (C=N, benzimidazole), 137–115 (Ar–C), 42 (CH_2), 35 (CH_2); ESI MS (*m/z*): 445 $[M+H]^+$. Anal. calcd. for $C_{21}H_{15}N_7O_3S$: C: 56.62, H: 3.39, N: 22.01; Found: C: 56.80, H: 3.38, N: 21.94%.

*1-((5-(4-Nitrophenyl)-1,3,4-oxadiazol-2-yl)methyl)-2-((pyrimidin-2-ylthio)methyl)-1H-benzo[d]imidazole (**5l**)*

Solid powder, dark brown; yield: 67%; m.p. (°C): 165–167; IR (KBr) cm^{-1}: 3015 (Ar–H), 2887 (C–H, CH_2), 1669 (C=N benzimidazole), 1570 (C=N pyrimidine), 1553 (C=C), 1536, 1458 (NO_2), 1360 (C–N), 1131 (C–O–C); ^1H NMR ($CDCl_3$): (δ ppm) 8.85 (2H, d, $J = 2.4$ Hz, pyr-H4, pyr-H6), 7.21 (1H, t, pyr-H5), 7.85–7.36 (m, 8H, Ar–H), 4.76 (s, 2H, CH_2), 4.23 (s, 2H, CH_2); ^{13}C NMR ($CDCl_3$): (δ ppm) 165, 162 (2C, oxadiazole), 151 (C=N, pyrimidine), 147 (C–NO_2), 140 (C=N, benzimidazole), 137–119 (Ar–C), 49 (CH_2), 40 (CH_2); ESI MS (*m/z*): 445 $[M+H]^+$. Anal. calcd. for $C_{21}H_{15}N_7O_3S$: C: 56.62, H: 3.39, N: 22.01; Found: C: 56.52, H: 3.40, N: 22.08%.

*2-(5-((2-((Pyrimidin-2-ylthio)methyl)-1H-benzo[d]imidazol-1-yl)methyl)-1,3,4-oxadiazol-2-yl)phenol (**5m**)*

Powder, dark green; yield: 72%; m.p. (°C): 242–244; IR (KBr) cm^{-1}: 3356 (Ar–O–H), 2995 (Ar–H), 2870 (C–H, CH_2), 1664 (C=N benzimidazole), 1568 (C=N pyrimidine), 1539 (C=C), 1375 (C–N), 1097 (C–O–C); ^1H NMR ($CDCl_3$): (δ ppm) 8.68 (2H, d, $J = 2.8$ Hz, pyr-H4, pyr-H6), 7.10 (1H, t, pyr-H5), 7.71–7.26 (m, 8H, Ar–H), 5.33 (s, 1H, OH, D_2O exchangeable), 4.91 (s, 2H, CH_2), 3.96 (s, 2H, CH_2); ^{13}C NMR ($CDCl_3$): (δ ppm) 170, 161 (2C, oxadiazole), 157 (C–OH), 156 (C=N, pyrimidine), 140 (C=N, benzimidazole), 134–118 (Ar–C), 50 (CH_2), 41 (CH_2); ESI MS (*m/z*): 417 $[M+H]^+$. Anal. calcd. for $C_{21}H_{16}N_6O_2S$: C: 60.56, H: 3.87, N: 20.18; Found: C: 60.80, H: 3.88, N: 20.10%.

*4-(5-((2-((Pyrimidin-2-ylthio)methyl)-1H-benzo[d]imidazol-1-yl)methyl)-1,3,4-oxadiazol-2-yl)phenol (**5n**)*

Solid, gray; yield: 70%; m.p. (°C): 212–214; IR (KBr) cm^{-1}: 3358 (Ar–O–H), 2980 (Ar–H), 2854 (C–H, CH_2), 1660 (C=N benzimidazole), 1568 (C=N pyrimidine), 1533 (C=C), 1379 (C–N), 1120 (C–O–C); ^1H NMR ($CDCl_3$): (δ ppm) 8.74 (2H, d, $J = 2.4$ Hz, pyr-H4, pyr-H6), 7.17

© 2014 WILEY-VCH Verlag GmbH & Co. KGaA, Weinheim

(1H, t, pyr-H5), 7.75–7.28 (m, 8H, Ar–H), 5.27 (s, 1H, OH, D_2O exchangeable), 4.95 (s, 2H, CH_2), 4.05 (s, 2H, CH_2); ^{13}C NMR ($CDCl_3$): (δ ppm) 169, 162 (2C, oxadiazole), 159 (C–OH), 156 (C=N, pyrimidine), 147 (C=N, benzimidazole), 138–117 (Ar–C), 49 (CH_2), 36 (CH_2); ESI MS (*m/z*): 417 $[M+H]^+$. Anal. calcd. for $C_{21}H_{16}N_6O_2S$: C: 60.56, H: 3.87, N: 20.18; Found: C: 60.72, H: 3.86, N: 20.14%.

*2-((Pyrimidin-2-ylthio)methyl)-1-((5-o-tolyl-1,3,4-oxadiazol-2-yl)methyl)-1H-benzo[d]imidazole (**5o**)*

Powder, green; yield: 64%; m.p. (°C): 196–198; IR (KBr) cm^{-1}: 2993 (Ar–H), 2867 (C–H, CH_2), 1673 (C=N benzimidazole), 1544 (C=N pyrimidine), 1530 (C=C), 1354 (C–N), 1132 (C–O–C); ^1H NMR ($CDCl_3$): (δ ppm) 8.80 (2H, d, $J = 2.4$ Hz, pyr-H4, pyr-H6), 6.98 (1H, t, pyr-H5), 7.82–7.16 (m, 8H, Ar–H), 4.59 (s, 2H, CH_2), 4.25 (s, 2H, CH_2), 2.27 (s, 3H, CH_3); ^{13}C NMR ($CDCl_3$): (δ ppm) 163, 160 (2C, oxadiazole), 156 (C=N, pyrimidine), 148 (C=N, benzimidazole), 135–113 (Ar–C), 136 (C–CH_3), 47 (CH_2), 40 (CH_2), 17 (CH_3); ESI MS (*m/z*): 415 $[M+H]^+$. Anal. calcd. for $C_{22}H_{18}N_6OS$: C: 63.75, H: 4.38, N: 20.28; Found: C: 63.96, H: 4.37, N: 20.20%.

*2-((Pyrimidin-2-ylthio)methyl)-1-((5-p-tolyl-1,3,4-oxadiazol-2-yl)methyl)-1H-benzo[d]imidazole (**5p**)*

Solid, brown; yield: 68%; m.p. (°C): 148–151; IR (KBr) cm^{-1}: 2997 (Ar–H), 2908 (C–CH_3), 2879 (C–H, CH_2), 1647 (C=N benzimidazole), 1561 (C=N pyrimidine), 1539 (C=C), 1390 (C–N), 1120 (C–O–C); ^1H NMR ($CDCl_3$): (δ ppm) 8.72 (2H, d, $J = 2.8$ Hz, pyr-H4, pyr-H6), 7.09 (1H, t, pyr-H5), 7.73–7.28 (m, 8H, Ar–H), 4.95 (s, 2H, CH_2), 4.29 (s, 2H, CH_2), 2.26 (s, 3H, CH_3); ^{13}C NMR ($CDCl_3$): (δ ppm) 169, 164 (2C, oxadiazole), 158 (C=N, pyrimidine), 149 (C=N, benzimidazole), 136–115 (Ar–C), 139 (C–CH_3), 48 (CH_2), 34 (CH_2), 22 (CH_3); ESI MS (*m/z*): 415 $[M+H]^+$. Anal. calcd. for $C_{22}H_{18}N_6OS$: C: 63.75, H: 4.38, N: 20.28; Found: C: 63.57, H: 4.39, N: 20.36%.

*1-((5-(2-Methoxyphenyl)-1,3,4-oxadiazol-2-yl)methyl)-2-((pyrimidin-2-ylthio)methyl)-1H-benzo[d]imidazole (**5q**)*

Amorphous solid powder, gray; yield: 73%; m.p. (°C): 235–237; IR (KBr) cm^{-1}: 3007 (Ar–H), 2887 (C–H, CH_2), 2848 (OCH_3), 1672 (C=N benzimidazole), 1565 (C=N pyrimidine), 1533 (C=C), 1358 (C–N), 1125 (C–O–C); ^1H NMR ($CDCl_3$): (δ ppm) 8.77 (2H, d, $J = 2.4$ Hz, pyr-H4, pyr-H6), 7.11 (1H, t, pyr-H5), 7.76–7.28 (m, 8H, Ar–H), 4.84 (s, 2H, CH_2), 4.17 (s, 2H, CH_2), 3.75 (s, 3H, OCH_3); ^{13}C NMR ($CDCl_3$): (δ ppm) 170, 166 (2C, oxadiazole), 159 (C=N, pyrimidine), 155 (<u>C</u>–OCH_3), 147 (C=N, benzimidazole), 137–114 (Ar–C), 56 (OCH_3), 48 (CH_2), 40 (CH_2); ESI MS (*m/z*): 431 $[M+H]^+$. Anal. calcd. for $C_{22}H_{18}N_6O_2S$: C: 61.38, H: 4.21, N: 19.52; Found: C: 61.56, H: 4.20, N: 19.58%.

*1-((5-(4-Methoxyphenyl)-1,3,4-oxadiazol-2-yl)methyl)-2-((pyrimidin-2-ylthio)methyl)-1H-benzo[d]imidazole (**5r**)*

Solid, brown; yield: 75%; m.p. (°C): 276–278; IR (KBr) cm^{-1}: 3012 (Ar–H), 2868 (C–H, CH_2), 2847 (OCH_3), 1664 (C=N benzimidazole), 1565 (C=N pyrimidine), 1551 (C=C), 1377 (C–N), 1139 (C–O–C); ^1H NMR ($CDCl_3$): (δ ppm) 8.66 (2H, d, $J = 2.8$ Hz, pyr-H4, pyr-H6), 7.19 (1H, t, pyr-H5), 7.80–7.25 (m, 8H, Ar–H), 4.85 (s, 2H, CH_2), 4.33 (s, 2H, CH_2), 3.78 (s, 3H, OCH_3); ^{13}C NMR ($CDCl_3$): (δ ppm) 164, 160 (2C, oxadiazole), 156 (C=N, pyrimidine), 151 (C–OCH_3), 147 (C=N, benzimidazole), 137–116 (Ar–C), 53 (O<u>C</u>H_3), 50 (CH_2), 41 (CH_2); ESI MS (*m/z*): 431 $[M+H]^+$. Anal. calcd. for $C_{22}H_{18}N_6O_2S$: C: 61.38, H: 4.21, N: 19.52; Found: C: 61.22, H: 4.22, N: 19.46%.

Biological activities

In vitro cyclooxygenase (COX) inhibition assay

Synthesized compounds (**5a–r**) were subjected to inhibit ovine COX-1 and human recombinant COX-2 using an enzyme immunoassay (EIA) kit as described previously [30]. Cyclooxygenase catalyzes the first step in the biosynthesis of arachidonic acid (AA) to PGH_2. $PGF_{2\alpha}$, produced from PGH_2 by reduction with stannous chloride, is measured by enzyme immunoassay. The assay was performed in duplicate according to the manufacturer's guidelines. The product of this enzymatic reaction produces a distinct yellow color that absorbs at 412 nm. The intensity of this color, determined spectrophotometrically, is proportional to the amount of PG tracer bound to the well, which is inversely proportional to the amount of PGs present in the well during the incubation. Percent inhibition was calculated by the comparison of compounds treated to various control incubations. The concentration of the test compounds that affords 50% inhibition of COX-2 (IC_{50}, μM) was calculated from the concentration inhibition response curve.

In vivo anti-inflammatory activity

Wistar albino rats (adult male), weighing 150–200 g, were used to determine anti-inflammatory activity. All animals were assigned into eight groups of six animals each. Animals were kept at 25–27°C and 30–70% relative humidity.

Selected compounds were assessed *in vivo* for their efficacy as anti-inflammatory agents by the method of Winter et al. [31]. The Group I served as control; received 0.5% w/v carboxymethylcellulose (CMC). Group II received standard drug indomethacin, at a dose level of 10 mg/kg and other groups received tested compounds, at a dose level of 50 mg/kg. The hind paw edema was induced in each rat by the sub-plantar injection of 0.1 mL of carrageenan suspension (1.0% w/v in 0.9% saline) 1 h after the administration of the tested compounds and standard drug orally. The volume of paw was measured by means of a digital plethysmometer (Panlab LE 7500) at 0, 3, and 4 h after the carrageenan injection. The percent edema inhibition was calculated in the control and treated animals according to the following equation:

$$\text{Percent edema inhibition} = \{1 - Vt/Vc\} \times 100$$

where V_c represents the mean increase in paw volume in the absence of tested compound (control) and V_t represents the mean increase of paw volume after treatment with the tested compound and standard drug.

Acute ulcerogenicity study

Potent compounds (**5b**, **5j**, and **5l**) were screened for acute ulcerogenecity according to the method of Cioli et al. [32]. The animals were fasted for 24 h before the experiment with free access to water and treated orally with two equal doses of either indomethacin (10 mg/kg, b.w.) or tested compounds (50 mg/kg, b.w.) at 0 and 12 h intervals, except the control group, which received 0.5% w/v CMC. After 17 h of the drug treatment, the rats were sacrificed. The stomach was removed and opened along the greater curvature, washed with distilled water, and cleaned gently by dipping in normal saline. The mucosal damage was examined by means of a microscope with a 4× magnifying lens. The mucosal damage in each stomach was assessed according to the following scoring system.

© 2014 WILEY-VCH Verlag GmbH & Co. KGaA, Weinheim

The mean score of each treated group minus the mean score of control group was regarded as severity index of gastric mucosal damage.

0.5 for redness; 1.0 for spot ulcers; 1.5 for hemorrhagic streaks; 2.0 for ulcers, more than 3 but less than 5; 3.0 for more than five ulcers.

Lipid peroxidation study

Lipid peroxidation in the gastric mucosa was determined according to the method of Ohkawa et al. [33]. After the evaluation of stomach for ulcers, the gastric mucosa of glandular portion was scrapped with the help of two glass slides, weighed (100 mg) and homogenized in 1 mL of a 0.15 M, ice-cold potassium chloride (KCl) solution and centrifuged at 3000 rpm for 10 min (REMI centrifuge). One milliliter of suspension was taken from the above tissue homogenate in test tube and 0.5 mL of 30% w/v trichloroacetic acid (TCA) was added to it, followed by 0.5 mL of 0.8% w/v TBA reagent. The tubes were then covered with aluminum foil and kept in water bath for 30 min at 80°C. After 30 min, tubes were taken out and kept in ice-cold water for 30 min and centrifuged at 3000 rpm for 15 min (R-BC DX REMI centrifuge). The absorbance of the supernatant was measured in spectrophotometer (UV-1601, SHIMADZU) at 540 nm against blank. Blank consisted of 1 mL of distilled water, 0.5 mL of 30% w/v TCA, and 0.5 mL of 0.8% w/v thiobarbituric acid (TBA). The results were expressed as nM of malondialdehyde (MDA) formed/h/mg of protein.

In vitro anticancer activity

All the selected compounds were submitted to NCI, USA for evaluating their *in vitro* anticancer activity at single dose (10 μM) against full NCI 60 human cell lines panels in accordance with their standard protocol. The compounds were added at a single concentration (10 μM) and the culture was incubated for 48 h. End point determinations were made with a protein binding dye, sulforhodamine B. The results for each compound were reported as percentage growth (GP %) of the treated cells and compared to the untreated control cells. Only significant results have been reported. Range of growth (%) showed the lowest and the highest growth that was found among different cancer cell lines. For NCI criteria, a compound which reduces the growth of any of the cell line by 32% or less is considered *in vitro* active [34].

Molecular docking study

The molecular docking study was carried out on 3D structure of cyclooxygenase 1 and 2 complex enzyme using Maestro 9.0 program (Schrodinger) by 64 bit operating system under Windows 7 with an HCl computer [Intel (R) Core (TM) i5-2400 CPU @ 3.10 GHz, 8GB memory]. The enzyme used in the study was taken from the Protein Data Bank (PDB ID: 1PGF for COX-1 and 6COX for COX-2), which has 95–97% similarity with the human cell enzyme and all active site residues in the vicinity of cofactor have exact counterparts and the structure was refined as follows [35, 36]. The enzyme structure was checked for missing atoms, bonds, and contacts. Water molecules and all residues other than ligand were manually deleted. The ligand molecules were constructed using the builder molecule and were energy minimized. The active site was generated using the grid box. The lowest energy conformation was selected and subjected to an energy minimization. The best binding modes of compound **5l** in the active site of 1PGF for COX-1 and 6COX for COX-2 are presented in Figs. 4 and 5.

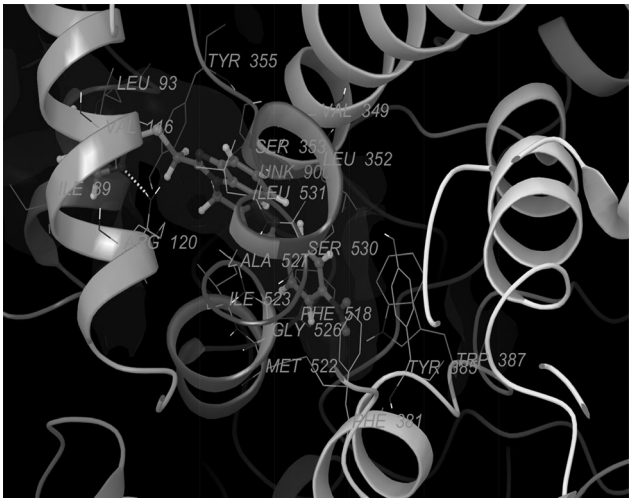

Figure 4. Binding mode of compound **5l** into the binding site of COX-1 (PDB code: 1PGF) showing hydrogen bond (dotted line) with Arg 120.

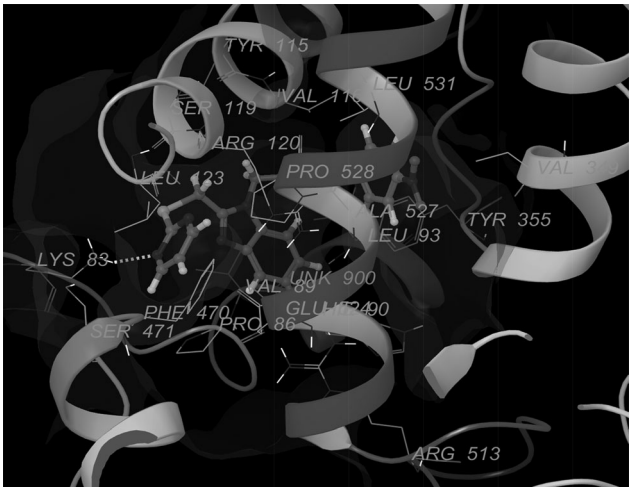

Figure 5. Binding mode of compound **5l** into the binding site of COX-2 (PDB code: 6COX) showing hydrogen bond (dotted line) with Lys 83.

Docking of compound **5l** into the active site of enzyme revealed that several molecular interactions (hydrogen bond, π interaction, and hydrophobic interactions) were considered to be responsible for the observed affinity of the compound. In contrast, compound **5l** lacks zwitter ion but it forms hydrogen bonds to the enzyme through its amino and carbonyl group with the Arg 120 (with COX-1) and Lys 83 (COX-2) residue, that is at the same residues where the natural inhibitors bind [35, 36]. Hydrogen bond interaction in COX-1 between the nitrogen (–N–) of the pyrimidine ring of the compound **5l** as it acts as a hydrogen bond donor with the carboxyl group (C=O) of the side chain residue of Arg 120 (1.94 Å) as it act as hydrogen bond acceptor. Hydrogen bond interaction in COX-2 between the

© 2014 WILEY-VCH Verlag GmbH & Co. KGaA, Weinheim

nitrogen (−N−) of the pyrimidine ring of the compound **5l** as it acts as a hydrogen bond donor with the carboxyl group (C=O) of the side chain residue of Lys 83 (2.12 Å) as it act as hydrogen bond acceptor (Figs. 4 and 5). The pyrimidine group of compound **5l** seems to have an important role in strong hydrogen bonding because the lone pair electrons on nitrogen atom of the ring delocalized into the compound. Pi–Pi interaction also play a crucial role in the inhibitory activity in COX-1, as appears between pyrimidine ring and phenyl ring of Arg 120 and formed CH−π interaction with Arg 120 (4.93 Å) as shown in Lig plot (Fig. 6). Pi–Pi interaction also play a crucial role in the inhibitory activity in COX-2, as appears between phenyl and imidazole ring of compound **5l** and phenyl ring of Try 355 and formed CH−π interaction with Try 355 (5.09 and 4.92 Å), form two more Pi–Pi interaction between phenyl ring (benzimidazole), phenyl ring of compound **5l**, and phenyl ring of Arg 120 (4.15 and 3.09 Å) as shown in Lig plot (Fig. 7). In addition to many hydrophobic interactions between the phenyl ring, oxadiazole, benzimidazole, and pyrimidine ring with the amino acids residues as shown in Figs. 6 and 7. For compound **5l**, calculated binding distance and binding energy (ΔGb) were 2.12 Å and −11.51 kcal/mol, respectively. The glide score value of compound **5l** with COX-1 and COX-2 was found to be −6.39 and −8.20, respectively, which indicates that compound **5l** interacts better with the COX-2 enzyme.

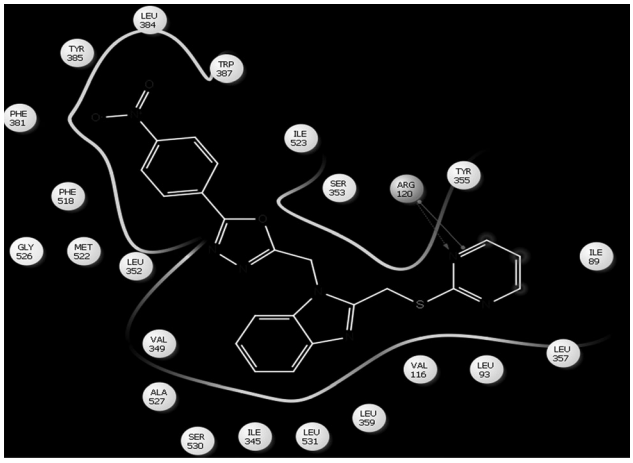

Figure 6. Lig plot of compound **5l** showing interaction into the binding sites of COX-1 enzyme (PDB code: 1PGF), hydrogen bond (pink dotted line) with Arg 120 (1.94 Å) and π–π interaction (green solid line) with Arg 120 (4.93 Å).

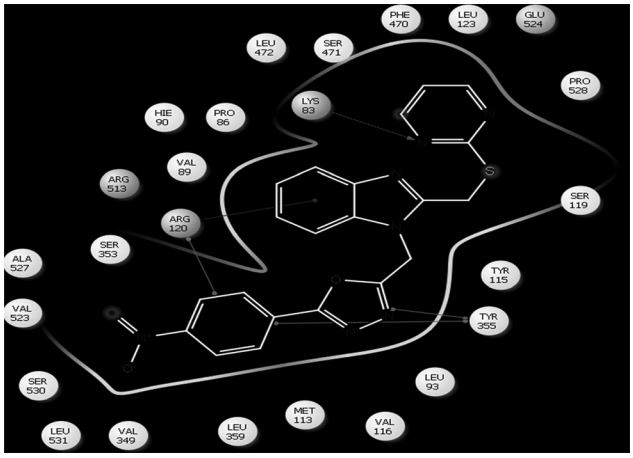

Figure 7. Lig plot of compound **5l** showing interaction into the binding sites of COX-2 enzyme (PDB code: 6COX), hydrogen bond (pink dotted line) with Lys 83 (2.12 Å) and π–π interaction (green solid line) with Tyr 355 (5.09 and 4.92 Å) and Arg 120 (4.15 and 3.09 Å).

The authors are grateful to Jamia Hamdard (Hamdard University), New Delhi, India for providing infrastructures and other facilities. The authors are also thankful to Council of Scientific and Industrial Research (CSIR), New Delhi, India for financial assistance in terms of SRF and National Cancer Institute (NCI), Chemotherapeutic Agents Repository, Fisher Bio Services, USA, for anticancer screening.

The authors have declared no conflict of interest.

References

[1] L. Ferrero-Miliani, O. H. Nielsen, P. S. Andersen, S. E. Girardin, *Clin. Exp. Immunol.* **2007**, *147*, 227–235.

[2] J. R. Vane, Y. S. Bakhle, R. M. Botting, *Ann. Rev. Pharmacol. Toxicol.* **1998**, *38*, 97–120.

[3] S. Fiorucci, R. Meli, M. Bucci, G. Cirino, *Biochem. Pharmacol.* **2001**, *62*, 1433–1438.

[4] C. J. Hawkey, *Lancet* **1999**, *353*, 307–314.

[5] L. Laine, *J. Pain Symptom Manage.* **2003**, *25*, S32–S40.

[6] K. Morwood, D. Gillis, W. Smith, F. Kette, *Int. Med. J.* **2005**, *35*, 240–246.

[7] M. Amer, V. R. Bead, J. Bathon, R. S. Blumenthal, D. N. Edwards, *Cardiol. Rev.* **2010**, *18*, 204–212.

[8] M. A. Hull, O. O. Faluyi, C. W. S. Ko, S. Holwell, D. J. Scott, R. J. Cuthbert, R. Poulsom, R. Goodlad, C. Bonifer, A. F. Markham, P. L. Coletta, *Carcinogenesis* **2006**, *27*, 382–391.

[9] J. Duque, M. D. Diaz-Munoz, M. Fresno, M. A. Iniguez, *Cell Signal.* **2006**, *18*, 1262–1269.

[10] Q. T. Zhao, S. Q. Yue, Z. Cui, Q. Wang, X. Cui, H. H. Zhai, L. H. Zhang, K. F. Dou, *Life Sci.* **2007**, *80*, 484–492.

[11] J. H. Chen, C. W. Wu, H. L. Kao, H. M. Chang, A. L. Y. Li, T. Y. Liu, C. W. Chi, *Cancer Lett.* **2006**, *239*, 263–270.

[12] B. S. Reddy, C. V. Rao, *J. Environ. Pathol. Toxicol. Oncol.* **2002**, *21*, 155–164.

[13] K. Krysan, K. L. Reckamp, S. Sharma, S. M. Dubinett, *Anti-Cancer Agents Med. Chem.* **2006**, *6*, 209–220.

[14] C. Iwata, M. R. Kano, A. Komuro, M. Oka, K. Kiyono, E. Johansson, Y. Morishita, M. Yashiro, K. Hirakawa, M. Kaminishi, K. Miyazono, *Cancer Res.* **2007**, *67*, 10181–10189.

[15] M. Gaba, D. Singh, S. Singh, V. Sharma, P. Gaba, *Eur. J. Med. Chem.* **2010**, *45*, 2245–2249.

[16] H. M. Refaat, *Eur. J. Med. Chem.* **2010**, *45*, 2949–2956.

[17] E. P. Jesudason, S. K. Sridhar, E. J. P. Malar, P. Shanmugapandiyan, M. Inayathullah, V. Arul, D. Selvaraj, R. Jayakumar, *Eur. J. Med. Chem.* **2009**, *44*, 2307–2312.

© 2014 WILEY-VCH Verlag GmbH & Co. KGaA, Weinheim

[18] R. Paramashivappa, P. P. Kumar, P. V. Subba Rao, A. S. Rao, *Bioorg. Med. Chem. Lett.* **2003**, *13*, 657–660.

[19] C. Michaux, X. de Leval, F. Julemont, J. M. Dogne, B. Pirotte, F. Durant, *Eur. J. Med. Chem.* **2006**, *41*, 1446–1455.

[20] L. Franke, E. Byvatov, O. Werz, D. Steinhilber, P. Schneider, G. Schneider, *J. Med. Chem. D* **2005**, *48*, 6997–7004.

[21] F. Perez-Cruz, S. Vazquez-Rodriguez, M. J. Matos, A. Herrera-Morales, F. A. Villamena, A. Das, B. Gopalakrishnan, C. Olea-Azar, L. Santana, E. Uriarte, *J. Med. Chem.* **2013**, *56*, 6136–6145.

[22] W. J. Song, X. D. Yang, X. H. Zeng, X. L. Xu, G. L. Zhang, H. B. Zhang, *RSC Adv.* **2012**, *2*, 4612–4615.

[23] S. L. Capim, G. M. Gonçalves, G. C. Dos Santos, B. G. Marinho, M. L. Vasconcellos, *Bioorg. Med. Chem.* **2013**, *21*, 6003–6010.

[24] M. U. Rahman, A. Rathore, A. A. Siddiqui, G. Parveen, M. S. Yar, *J. Enzyme Inhib. Med. Chem.* **2014**, *21*, 1–11.

[25] M. Schiffmann, H. Sticht, C. Korth, *BioDrugs* **2012**, *26*, 21–31.

[26] A. Husain, M. Rashid, R. Mishra, S. Parveen, D. S. Shin, D. Kumar, *Bioorg. Med. Chem. Lett.* **2012**, *22*, 5438–5444.

[27] H. Skolnik, J. G. Miller, A. R. Day, *J. Am. Chem. Soc.* **1943**, *65*, 1854–1858.

[28] M. Cowart, S. P. Latshaw, P. Bhatia, J. F. Daanen, J. Rohde, S. L. Nelson, M. Patel, T. Kolasa, M. Nakane, M. E. Uchic, L. N. Miller, M. A. Terranova, R. Chang, D. L. Donnelly-Roberts, M. T. Namovic, P. R. Hollingsworth, B. R. Martino, J. J. Lynch, J. P. Sullivan, G. C. Hsieh, R. B. Moreland, J. D. Brioni, A. O. Stewart, *J. Med. Chem.* **2004**, *47*, 3853–3864.

[29] H. T. A. Mohsen, F. A. F. Raga, M. M. Ramla, H. I. Diwani, *Eur. J. Med. Chem.* **2010**, *45*, 2336–2344.

[30] M. J. Uddin, P. N. P. Rao, R. McDonald, E. E. Knaus, *J. Med. Chem.* **2004**, *47*, 6108–6111.

[31] A. Winter, E. A. Risley, G. W. Nuss, *Proc. Soc. Exp. Biol. Med.* **1962**, *111*, 544–547.

[32] V. Cioli, S. Putzolu, V. Rossi, S. P. Barcellona, C. Corradino, *Toxicol. Appl. Pharmacol.* **1979**, *50*, 283–289.

[33] H. Ohkawa, N. Ohishi, K. Yagi, *Anal. Biochem.* **1979**, *95*, 351–358.

[34] P. Corona, A. Carta, M. Loriga, G. Vitale, G. Paglietti, *Eur. J. Med. Chem.* **2009**, *44*, 1579–1591.

[35] P. J. Loll, D. Picot, O. Ekabo, R. M. Garavito, *Biochemistry* **1996**, *35*, 7330–7340.

[36] R. G. Kurumbail, A. M. Stevens, J. K. Gierse, J. J. McDonald, R. A. Stegeman, J. Y. Pak, D. Gildehaus, J. M. Miyashiro, T. D. Penning, K. Seibert, P. C. Isakson, W. C. Stallings, *Nature* **1996**, *384*, 644–648.

© 2014 WILEY-VCH Verlag GmbH & Co. KGaA, Weinheim